A Growth Model of Single Crystalline Hollow Spheres: Oriented Attachment of Cu 2 O Nanoparticles to the Single Crystalline Shell Wall

ARTICLE *in* CRYSTAL GROWTH & DESIGN · OCTOBER 2008

Impact Factor: 4.89 · DOI: 10.1021/cg800258n

3 AUTHORS, INCLUDING:

Haolan Xu
University of South Australia
48 PUBLICATIONS **2,546** CITATIONS
SEE PROFILE

Wenzhong Wang
Minzu University of China
212 PUBLICATIONS **7,689** CITATIONS
SEE PROFILE

CRYSTAL GROWTH & DESIGN
2008
VOL. 8, NO. 10
3486–3489

Communications

A Growth Model of Single Crystalline Hollow Spheres: Oriented Attachment of Cu_2O Nanoparticles to the Single Crystalline Shell Wall

Haolan Xu, Wenzhong Wang,* and Lin Zhou

State Key Laboratory of High Performance Ceramics and Superfine Microstructure, Shanghai Institute of Ceramics, Chinese Academy of Sciences, 1295 DingXi Road, Shanghai 200050, P. R. China

Received March 11, 2008; Revised Manuscript Received July 17, 2008

ABSTRACT: A growth mechanism for single crystalline hollow spheres was proposed based on the study of the formation process of single crystalline Cu_2O multishelled hollow spheres. On the basis of transmission electron microscopy, high resolution transmission electron microscopy, selected area electron diffraction analysis of the product collected at different formation stages, it is found that the nanoparticles with a size of 2−5 nm first formed well-crystallized porous shelled hollow spheres via oriented attachment, and then the porous shells were further crystallized and became compact by Ostwald ripening to form well-crystallized hollow spheres.

Shape controlled synthesis of nanomaterials has spurred great interest owing to their attractive morphology-dependent properties.[1−7] To achieve this aim, the study of the growth mechanism of various shaped nanomaterials is fundamentally important, which will further guide the shape controlled synthesis along with morphology-dependent properties and applications. In the past decade, hollow spheres were widely studied due to their unique structures and potentially promising applications.[8−14] However, because most reported hollow spheres are all with a polycrystalline shell wall, this may degrade the structural stability of the hollow structures. Very recently, some hollow structures with a single crystalline shell wall were prepared successfully, such as single crystalline PbS, Cu_2O, CuS, and Fe_3O_4 hollow spheres,[14−17] which is important for the extension of their potential applications. Furthermore, they provided excellent models to study the crystal growth of the single crystalline hollow structures. The study of the mechanism of the single crystalline shell wall of the hollow structure seems necessary. So far as we know, among the various mechanisms for hollow structures, such as mass diffusion obeying Fick's first law,[18] solid evacuation with Ostwald ripening,[19] self-assembly,[20,21] and the Kirkendall effect,[17,22] it seems that the Kirkendall effect could lead to single crystalline hollow structures.[17] However, the Kirkendall mechanism can be ruled out in many cases[14−16] because there is only one phase in the system. This inspired us to study the growth mechanism for the formation of single crystalline hollow spheres to shed light on other potential growth mechanisms for the single crystalline shell wall. Herein, based on our previous work on Cu_2O multishelled hollow spheres (MHS) with a single crystalline shell wall, we carefully investigated the detailed formation process of the single crystalline shell wall as well as the multilayered structure.[14] A combined crystal growth mechanism, oriented attachment followed by Ostwald ripening, is proposed for the formation of Cu_2O hollow spheres with a single crystalline shell wall. Previously, the oriented attachment growth mechanism has been mainly illustrated in the growth of well, single-crystallized one-, two-, and three-dimensional (1D, 2D, and 3D) solid structures.[23−36] Herein, we introduce it into the formation of well-crystallized hollow structures. This will be helpful for understanding the growth behavior of the single crystalline hollow spheres.

Cu_2O MHS were prepared according to the literature.[14] To investigate the formation process of the single crystalline shell wall, a series of experiments were carried out to capture the intermediate states of the crystal growth. In a typical procedure, 0.05 g of $CuSO_4 \cdot 5H_2O$ was dissolved in 100 mL of CTAB solution. The concentration of CTAB was 0.13 M. 0.18 g of ascorbic acid was then added and the solution was heated to 60 °C and kept at the temperature for 20 min. The diluted NaOH (0.05 M) solution was used and added at a rate of 0.1 mmol/min. A yellow precipitate was produced. The samples were collected 10, 30, 50 s after the appearance of yellow precipitate separately. It is found that the reaction (Cu^{2+} reduced into Cu_2O) proceeded and finished quickly when the pH reaches a certain value. Thus, diluted NaOH solution (0.05 M) was used to slow down the reaction rate to capture the intermediate state. In addition, the primary state of newly generated Cu_2O (10 s sample) is soluble in the hot solution (60 °C) and will dissolve immediately after sampling, which makes it difficult to capture the early stage of the formation process. In our experiment, we harvested the suspension (10 s sample) and injected it into ethanol with a temperature of −3 °C immediately to keep the primary state. Then the samples were centrifuged, washed sequentially with deionized water and ethanol several times, and dried at 50 °C for 5 h under a vacuum. Other samples were directly centrifuged, washed, and dried. Transmission electron microscopy (TEM) images and high-resolution TEM (HRTEM) images were

* Corresponding author. E-mail: wzwang@mail.sic.ac.cn.

10.1021/cg800258n CCC: $40.75
Published on Web 08/29/2008

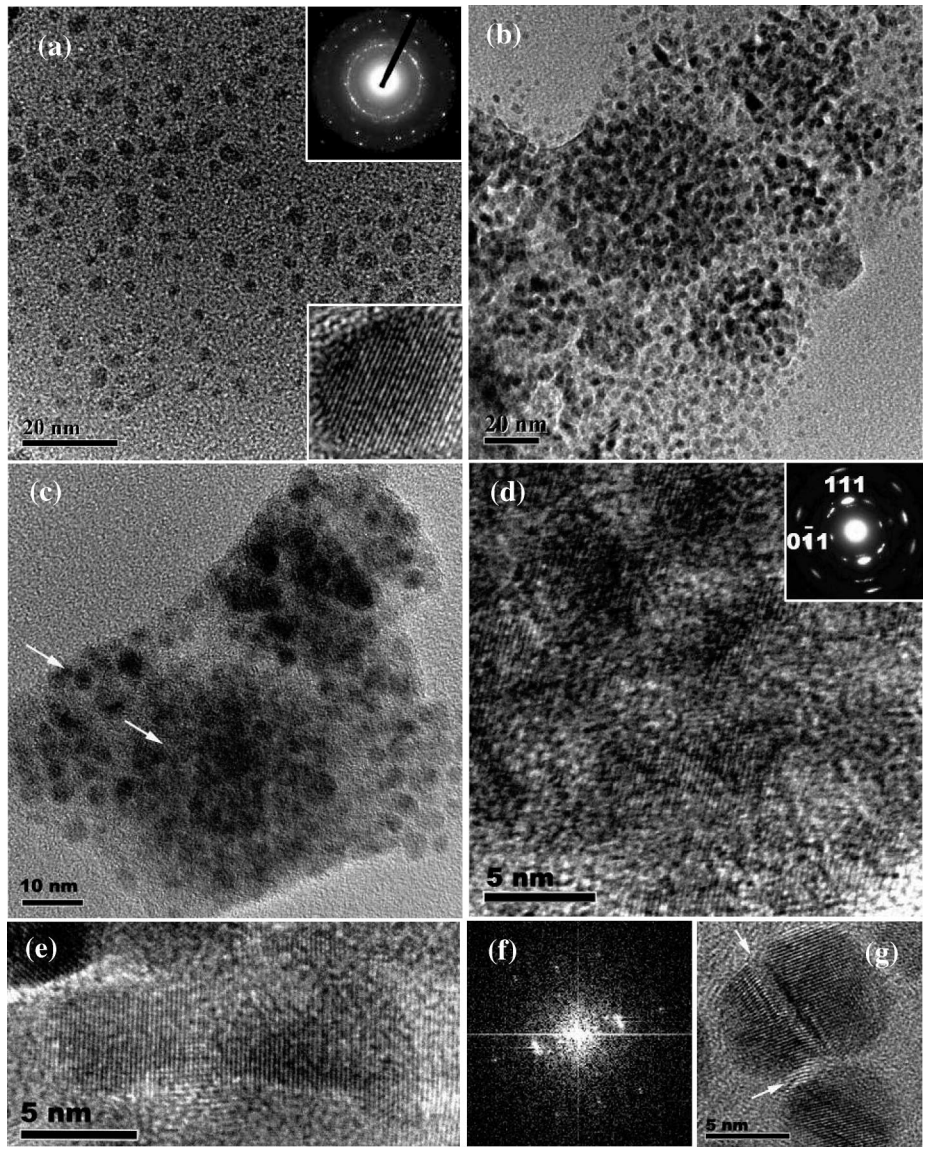

Figure 1. TEM images of the product collected at an early stage, 10 s after the appearance of yellow precipitate: (a) dispersed Cu_2O nanoparticles, top inset is the SAED pattern, bottom inset is a HRTEM image of a single Cu_2O nanoparticle; (b) aggregating Cu_2O nanoparticles; (c) primary aggregation of Cu_2O nanoparticles for multishells; (d) HRTEM image of aggregated Cu_2O nanoparticles and the corresponding SAED pattern (inset); (e) HRTEM image of orientedly attached Cu_2O nanoparticles and (d) the corresponding Fourier transform pattern; (e) HTREM image of 3 orientedly attached Cu_2O nanoparticles.

recorded by a JEOL JEM-2100F field emission transmission electron microscope, using an accelerating voltage of 200 kV.

Figure 1 records the morphology of the product collected 10 s after the color turned from colorless to yellow (denoted as 10 s sample), from which original Cu_2O nanoparticles with a size about 2−5 nm are observed (Figure 1a). The HRTEM image (low inset in Figure 1a) shows an individual Cu_2O nanocrystal, indicating it is single crystalline in structure. The SAED pattern (up inset in Figure 1a) shows the polycrystalline nature of a number of Cu_2O nanoparticles which indicates the random orientation of their crystal planes. These Cu_2O nanoparticles serve as the primary units for the construction of Cu_2O hollow spheres. They aggregate on the surfaces of CTAB vesicles (Figure 1b). From Figure 1c one can see the original outline of the MHS; the arrowed part may evolve into different shell walls. More examples are shown in the Supporting Information (Figure S1a,c). The Cu_2O nanoparticles

Scheme 1. Schematic Illustration of the Formation of Well Crystalline Shell Wall of the Multishelled Cu_2O Hollow Spheres (Partial View of the Shell)

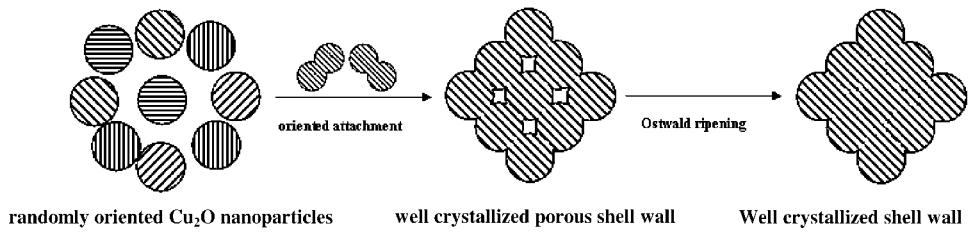

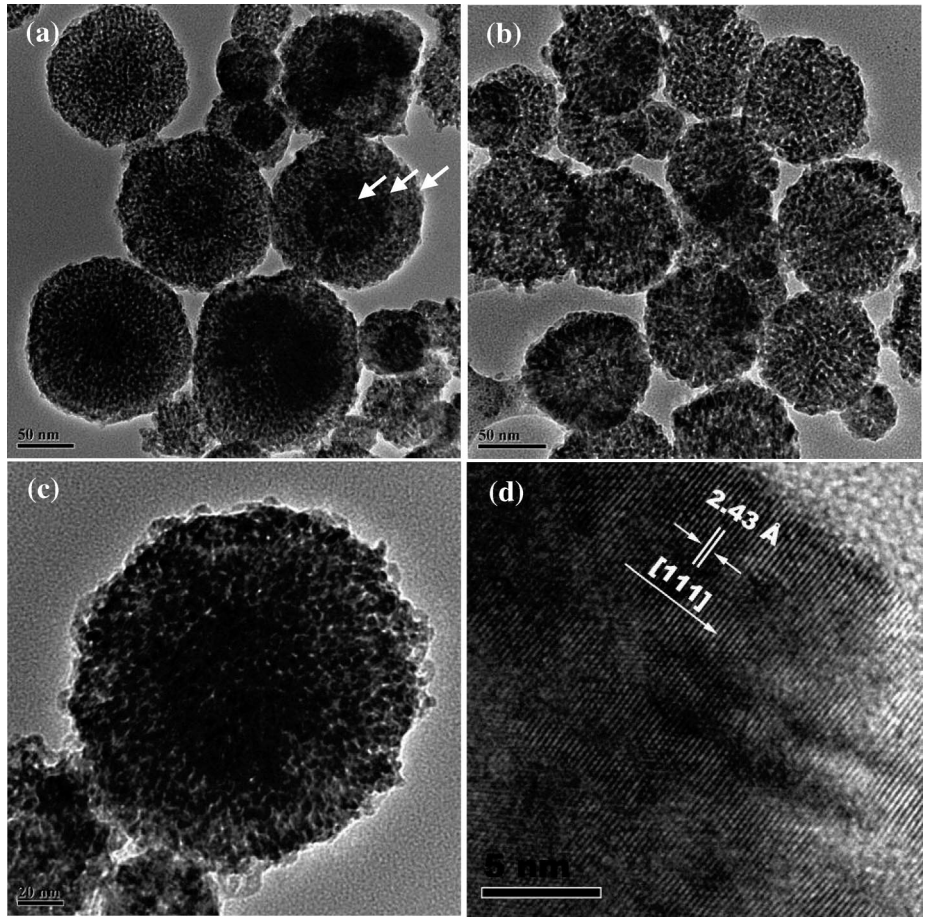

Figure 2. TEM images of the product collected 30 s after the appearance of the yellow precipitate: (a), (b), (c) the integrated porous MHS; (d) HRTEM image of a porous MHS.

dispersed around the outside of the hollow spheres are randomly oriented as shown in the HRTEM image (Supporting Information, Figure S1b), which agrees well with the conclusion from the SAED pattern (up inset in Figure 1a). These Cu_2O nanoparticles then orientedly aggregated into primary Cu_2O porous-shelled hollow spheres as shown in Figure 1d (for more examples see Supporting Information, Figure S1d). The HRTEM image and the corresponding SAED pattern demonstrate that the Cu_2O nanoparticles aggregated by oriented attachment of their (111) planes. Compared with the dispersed Cu_2O nanoparticles, this aggregated structure is well oriented and crystallized. The crystal planes are discontiguous attributed to the pores but still with accordant orientation, and some unconspicuous outlines of Cu_2O particles are still distinguishable. Therefore, it is concluded that, in this early stage, oriented attachment plays a key role in the formation of the porous shell wall of MHS. Cu_2O nanoparticles aggregate and orientedly attach into porous-shelled Cu_2O hollow spheres. Figure 1e shows the attached Cu_2O particles, from which one can see that the lattice planes of the attached particles are almost perfectly aligned. The corresponding Fourier transform pattern (Figure 1f) indicates that the attached structure is single crystalline. Three attached Cu_2O nanoparticles are demonstrated in Figure 1g; the arrowed part is the boundary of the particles. This partial 2D oriented attachment of Cu_2O nanoparticles on the surfaces of the CTAB vesicles (template) will produce the porous shell wall of MHSs, because as illustrated in Scheme 1, the attachment of spherical particles will obviously remain in the interspaces between the particles due to geometrical factors. This oriented aggregation of nanoparticles into 3D porous-shelled hollow spheres via oriented attachment was rarely reported. Furthermore, it is believed that this porous-shelled structure is the key factor for the formation of MHS, because this particular structure permits the rapid penetration of the reactants from the outside to the inside for the further reactions.

The morphology and structure of the product collected 30 s after the appearance of the yellow precipitate (30 s sample) are demonstrated in Figure 2. After the foregoing oriented aggregation of Cu_2O nanoparticles on the surface of CTAB vesicles in the earlier stage described above, integrated porous single-shelled and multishelled hollow spheres are formed. The primary structure of the MHSs is clearly revealed in Figure 2a−c, in which different layers of the shell are distinguishable (arrowed part). HRTEM image (Figure 2d) shows the well-crystallized porous shell wall of these hollow structures. The average interfringe distance is measured to be about 2.43 Å, which could be assigned to (111) planes of cubic Cu_2O. SAED patterns of different structured porous Cu_2O hollow spheres confirm the well-crystallized structures (Supporting Information, Figure S2). Therefore, we can conclude that in the first step Cu_2O nucleate followed by the oriented aggregation at the interface of the CTAB vesicles. The well-crystallized porous framework of the multishelled hollow sphere is formed in this step. This well-crystallized porous framework serves as the base structure for the final single crystalline MHSs. Cu^{2+} and OH^- could penetrate through these porous shells, which allows the Ostwald ripening of the inner shell wall to form the compact shell wall. In addition, we can stop the reaction at this stage to obtain these multishelled Cu_2O hollow spheres with larger numbers of pores, which may possess a larger surface area and higher ion exchange activity than that of the final product of MHSs with a compact shell wall.

After the formation of these well-crystallized porous shell walls, Ostwald ripening plays a key role in the next densification (Scheme 1) of this porous shell wall to achieve the final MHSs with a well-crystallized shell wall (Figure 3c). TEM images (Figure 3a−c)

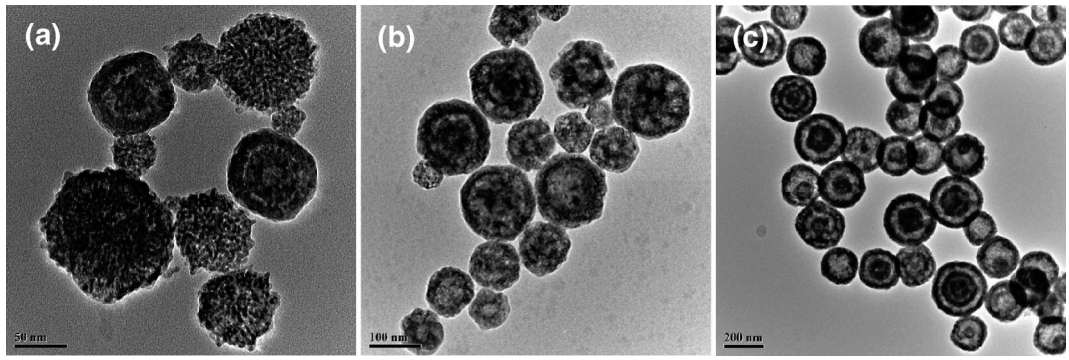

Figure 3. TEM images illustration of the densification of the porous-shelled hollow spheres: (a) the coexistence of the porous-shelled hollow spheres and the relative compact hollow spheres in the 30 s sample; (b) the relative compact hollow spheres in the 50 s sample; (c) final multishelled hollow spheres.

illustrate the densification process of the porous-shelled hollow spheres. In the 30 s sample (Figure 3a), we can see that some relative compact hollow spheres coexist with the porous-shelled hollow spheres. Then, pores in the shell wall gradually disappeared, and the compact solid shell wall formed accompanying Ostwald ripening. Figure 3b shows the 50 s sample, from which one can see that the shell walls of all Cu_2O hollow spheres are relatively compact.

In summary, we successfully captured the intermediate state for the formation of a multishelled structure as well as the single crystalline shell wall by controlling the experiments, and a combined growth mechanism of oriented attachment followed by Ostwald ripening is proposed for the formation of multishelled single crystalline hollow spheres. In the first stage, Cu_2O nanoparticles (2−5 nm) undergo a 2D oriented attachment under the direction of CTAB multilamellar vesicles to form the primary well-crystallized porous-shelled hollow spheres, which serves as the base framework for the single crystalline MHSs. In the second stage, densification of this porous shell wall via Ostwald ripening takes place to achieve compact multishelled hollow spheres with single crystalline shell wall. Remarkably, the formation of the porous shell wall is important to the multishelled hollow spheres by providing exchanging channels for reactants. The finding reveals the formation mechanism of the single crystalline shell wall of the Cu_2O hollow spheres, which may serve as one of the general growth mechanisms for the single crystalline hollow structure and prove helpful for understanding and controlling the growth behavior of hollow structures.

Acknowledgment. Financial support from the National Natural Science Foundation of China (No. 50672117) and National Basic Research Program of China (973 Program, 2007CB613302) is gratefully acknowledged.

Supporting Information Available: TEM images of the 10 s sample; TEM images and the corresponding SAED patterns of the Cu_2O porous-shelled hollow spheres (30 s sample). This information is available free of charge via the Internet at http://pubs.acs.org.

References

(1) Alivisatos, A. P. *Science* **1996**, *271*, 933.
(2) El-Sayed, M. A. *Acc. Chem. Res.* **2001**, *34*, 257.
(3) Hu, J. T.; Odom, T. W.; Liber, C. M. *Acc. Chem. Res.* **1999**, *32*, 435.
(4) Burda, C.; Chen, X. B.; Narayanan, R.; El-Sayed, M. A. *Chem. Rev.* **2005**, *105*, 1025.
(5) Xia, Y. N.; Yang, P. D.; Sun, Y. G.; Wu, Y. Y.; Mayers, B.; Gates, B.; Yin, Y. D.; Kim, F.; Yan, H. Q. *Adv. Mater.* **2003**, *15*, 353.
(6) Kumar, S.; Nann, T. *Small* **2006**, *2*, 316.
(7) Xu, H. L.; Wang, W. Z.; Zhu, W. *J. Phys. Chem. B* **2006**, *110*, 13829.
(8) Caruso, F.; Caruso, R. A.; Möhwald, H. *Science* **1998**, *282*, 1111.
(9) Caruso, F. *Chem. Eur. J.* **2000**, *6*, 413.
(10) Caruso, F. *Adv. Mater.* **2001**, *13*, 11.
(11) Göltner, C. G. *Angew. Chem., Int. Ed.* **1999**, *38*, 3155.
(12) Zhong, Z. Y.; Yin, Y. D.; Gates, B.; Xia, Y. N. *Adv. Mater.* **2000**, *12*, 206.
(13) Sun, Y. G.; Xia, Y. N. *Science* **2002**, *298*, 2176.
(14) Xu, H. L.; Wang, W. Z. *Angew. Chem., Int. Ed.* **2007**, *46*, 1489.
(15) Zhu, L. P.; Xiao, H. M.; Zhang, W. D.; Yang, G.; Fu, S. Y. *Cryst. Growth Des.* **2008**, *8*, 957.
(16) Zhao, P. T.; Wang, J. M.; Chen, G.; Xiao, Z.; Zhou, J.; Chen, D.; Huang, K. X. *J. Nanosci. Nanotechnol.* **2008**, *8*, 379.
(17) Cao, H. L.; Qian, X. F.; Wang, C.; Ma, X. D.; Yin, J.; Zhu, Z. K. *J. Am. Chem. Soc.* **2005**, *127*, 16024.
(18) Xu, H. L.; Wang, W. Z.; Zhu, W.; Zhou, L. *Nanotechnology* **2006**, *17*, 3649.
(19) Yang, H. G.; Zeng, H. C. *J. Phys. Chem. B* **2004**, *108*, 3492.
(20) Park, S.; Lim, J. -H.; Chung, S. -W.; Mirkin, C. A. *Science* **2004**, *303*, 348.
(21) Yang, H. G.; Zeng, H. C. *Angew. Chem., Int. Ed.* **2004**, *43*, 5930.
(22) Yin, Y. D.; Rioux, R. M.; Erdonmez, C. K.; Hughes, S.; Somorjai, G. A.; Alivisatos, A. P. *Science* **2004**, *304*, 711.
(23) Zhang, J.; Wang, Y. H.; Zheng, J. S.; Huang, F.; Chen, D. G.; Lan, Y. Z.; Ren, G. Q.; Lin, Z.; Wang, C. *J. Phys. Chem. B* **2007**, *111*, 1449.
(24) Zhang, J.; Lin, Z.; Lan, Y. Z.; Ren, G. Q.; Chen, D. G.; Huang, F.; Hong, M. C. *J. Am. Chem. Soc.* **2006**, *128*, 12981.
(25) Teo, J. J.; Chang, Y.; Zeng, H. C. *Langmuir* **2006**, *22*, 7369.
(26) Geng, J.; Lu, D. J.; Zhu, J. J.; Chen, H. Y. *J. Phys. Chem. B* **2006**, *110*, 13777.
(27) Zeng, H. C. *J. Mater. Chem.* **2006**, *16*, 649.
(28) Burleson, D. J.; Penn, R. L. *Langmuir* **2006**, *22*, 402.
(29) Cheng, Y.; Wang, Y. S.; Zheng, Y. H.; Qin, Y. *J. Phys. Chem. B* **2005**, *109*, 11548.
(30) Xu, H. L.; Wang, W. Z.; Zhu, W.; Zhou, L.; Ruan, M. L. *Cryst. Growth Des.* **2007**, *7*, 2720.
(31) Liu, B.; Yu, S. H.; Li, L. J.; Zhang, F.; Zhang, Q.; Yoshimura, M.; Shen, P. K. *J. Phys. Chem. B* **2004**, *108*, 2788.
(32) Huang, F.; Zhang, H. Z.; Banfield, J. F. *Nano Lett.* **2003**, *3*, 373.
(33) Banfield, J. F.; Welch, S. A.; Zhang, H.; Ebert, T. T.; Peen, R. L. *Science* **2000**, *289*, 751.
(34) Peen, R. L.; Banfield, J. F. *Science* **1998**, *281*, 969.
(35) Peen, R. L.; Banfield, J. F *Geochim. Cosmochim. Acta* **1999**, *63*, 1549.
(36) Pacholski, C.; Kornowski, A.; Weller, H. *Angew. Chem., Int. Ed.* **2002**, *41*, 1188.

CG800258N